

Effect of Cluster Surface Energies on Secondary-Ion-Intensity Distributions from Ionic Crystals

J. E. Campana, T. M. Barlak, R. J. Colton, J. J. DeCorpo, J. R. Wyatt, and B. I. Dunlap
Chemistry Division, Naval Research Laboratory, Washington, D. C. 20375

(Received 22 June 1981)

Ultrahigh-mass cluster ions ($m/z > 18\,000$) of the type $[M(MX)_n]^+$ have been produced by xenon-ion bombardment of CsI and detected by a high-performance secondary-ion mass spectrometer. The mass spectra (ion intensity versus n) show anomalous behavior which is correlated with hypothesized dominance of cubiclike clusters having low surface energies.

PACS numbers: 36.40.+d, 07.75.+h, 35.20.Wg

Vapor-phase alkali-halide clusters are widely studied systems because of their elementary electronic properties, ionic nature, and low vapor pressure. Surprisingly, after almost thirty years of research on the gaseous alkali-halide aggregates,¹ the thermodynamic, structural, and electronic properties of almost all clusters, even most dimers, are unknown.² Investigations have been restricted to the smaller gaseous aggregates, typically dimers, trimers, and tetramers, because of limitations in instrumentation and in methods of cluster production. Several instrumental techniques including Knudsen-cell mass spectrometry,³ matrix isolation methods,⁴ and more recently photoelectron spectroscopy^{5,6} and secondary-ion mass spectrometry (SIMS)^{7,8} have been used to investigate properties of relatively small, gaseous alkali-halide aggregates. Theoretical methods are also being developed to study structural and electronic properties of alkali-halide clusters.^{9,10}

Ion bombardment of crystalline alkali halides (MX) in SIMS produces cluster ions of the type $[M(MX)_n]^+$ and $[X(MX)_n]^-$, where, for example, clusters up to $n=3$ have been observed in the positive-ion mass spectrum of CsI and up to $n=13$ in NaF.⁸ Mass spectra of various alkali halides show a power-law dependence of ion intensity on cluster size or n value over the mass ranges accessible with conventional SIMS instruments.⁸

Recently, we described a high-performance secondary-ion mass spectrometer,¹¹ based on a double-focusing (Mattauch-Herzog geometry) mass analyzer. This instrument has superior performance characteristics relative to the conventional SIMS instruments based on the quadrupole mass filter. Our high-performance instrument is relatively free from adverse mass-discrimination effects and has a wide energy band-pass (16 eV per 1000 eV secondary ions). The mass range is limited only by the maximum mag-

netic field (1.1 T) and the secondary-ion extraction and transmission efficiencies at low accelerating voltages, since the mass range is inversely proportional to the accelerating voltage (e.g., mass-to-charge ratio $m/z = 1-5400$ at 1 kV).

We have studied a number of metal halides with this instrument in order to elucidate the cluster-ion formation process and the sputtered ion emission mechanism.¹² We have discovered high-mass alkali-iodide ions far beyond those accessible to conventional SIMS instruments. For these high-mass ions, the nonmonotonic distribution of ion intensity with cluster size (n) gives insight into the three-dimensional structure of the high-mass cluster species. We interpret our results by the simplest model of the sputter ejection process—the bond-breaking model.^{13,14} However, our considerations, appropriately modified, are relevant in the more sophisticated models being developed.^{15,16}

Our most recent investigation of alkali iodides bombarded with 4.0–4.7 keV xenon ions¹⁷ has yielded CsI mass spectra of cluster ions of the type $[Cs(CsI)_n]^+$ extending beyond $m/z = 18\,000$ or cluster sizes up to $n=70$. This n value is more than twenty times greater than CsI cluster ions previously reported in SIMS studies.⁸ Figure 1 summarizes the CsI data obtained in our experiments by xenon-ion bombardment of an infrared-type CsI pellet (spectroscopic grade CsI powder pressed at 1.4×10^6 N/m²). A continuous-dynode particle multiplier coupled to a pulse-counting system capable of measurement over six orders of magnitude is utilized in our system for ion-abundance measurements.

While the ion-to-electron conversion process (kinetic versus potential emission) of the particle multiplier is expected to affect ion-abundance measurements, we have shown that these do not have an effect on the relative intensity measurements above the first two or three n values. Differences in relative ion intensities have been

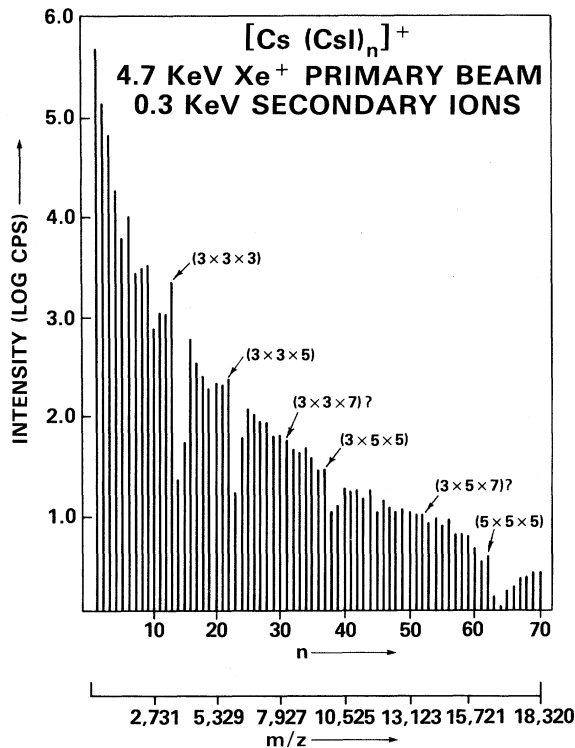


FIG. 1. Ultrahigh-mass SIMS spectrum of CsI at 300 V accelerating voltage. The structures of the species corresponding to $n = 13, 22, 31, 37, 52,$ and 62 are attributed to low-surface-energy cluster geometries.

noted with this system¹⁸ about the velocity threshold for kinetic emission¹⁹ (5.5×10^4 m/s) for NaI at 500-V ($n = 1, 2$), 1-kV ($n = 2, 3$), and 3-kV ($n = 3, 4$) accelerating voltages between the ion clusters shown in parentheses. A more thorough discussion of ion-to-electron conversion¹² and ion-abundance measurements of cluster species^{12, 20} will be presented elsewhere.

Intensity anomalies are observed in the regions $n = 13-15$, $n = 22-24$, $n = 37-39$, and $n = 62-64$, and, less dramatically, at $n = 31-33$ and $n = 52-54$. Intensity anomalies have also been observed at $n = 13-15$ for RbI, KI, and NaI and at $n = 22-24$ for KI and NaI.¹² Ion intensities at these n values are atypical because the ion intensity of the first n value in the set is enhanced relative to the previous n value while the two ion intensities immediately following the first n value are distinctly less intense or below the detectable limit. This nonmonotonic trend is not expected on the basis of previous experimental results, where the overall plot of $\log(\text{intensity})$ vs $\log n$ decreases linearly.⁸

We attribute the enhanced ion intensities at $n = 13, 22, 37,$ and 62 , evident in Fig. 1, to the occurrence and possible dominance of a few extraordinarily compact cluster geometries. These are "crystallites" having a low surface energy²¹ or equivalently a high ratio of total nearest-neighbor bonds to total atoms. Such clusters have a minimum number of facets of nearly equal areas. (The effect of cluster surface energies on binding-energy trends and other cluster properties has been studied.⁹) We now give qualitative statistical and energetic arguments favoring this interpretation.

First, consider a simple nearest-neighbor bond-breaking picture. Let β be the probability that a given bond is broken, and hence $1 - \beta$ the probability that it is not broken. Additionally, we assume that β is constant over some volume—the primary-ion impact zone. A more complete solution of this model is under investigation; however, its major consequences are illustrated by considering two extreme cluster geometries that might arise upon shattering a simple-cubic crystal. One extreme is the linear array, possibly with kinks, but with each atom bonded to two nearest neighbors (linear polymer). In the simple-cubic structure each atom is bonded to six nearest neighbors; thus, within this model, each such linear configuration occurs with probability

$$P_N(\text{linear}) = \beta^{4N+2}(1 - \beta)^{N-1}, \quad (1)$$

where N is the number of atoms in the configuration. For a 27-atom linear array ($n = 13$) we have

$$P_{27}(\text{linear}) = \beta^{110}(1 - \beta)^{26}. \quad (2)$$

At the other extreme of 27-atom cluster geometries is the $3 \times 3 \times 3$ cubic structure. It occurs with probability

$$P_{27}(\text{cube}) = \beta^{54}(1 - \beta)^{54}. \quad (3)$$

For our assumption of constant β to be approximately valid, bond breaking must occur over a significant volume. In this case, energy conservation (applied to the kinetic energy of the primary ion) requires that β be small. Furthermore, a large β is inconsistent with the occurrence of large clusters. In the small- β limit the 27-atom cubic cluster is β^{-56} more probable than any linear cluster. However, the degree to which the cubic configuration dominates all other configurations in this model can only be determined via a complete treatment involving enumeration of all configurations which contain 27 atoms. The identical enumeration roadblock exists in percola-

tion theory.²² Nevertheless, sufficient computational studies have been performed to show that for β below the critical value for the appearance of the infinite cluster, the finite clusters are compact.

For ionic crystals such as CsI, the nearest-neighbor description of bonding is somewhat inappropriate because of the long range of electrostatic interactions, which, in effect, renormalize the nearest-neighbor Coulomb attractions by a factor varying from unity to the Madelung constant with increasing cluster size. For these crystals, a picture involving cleaving rather than bond breaking is more appropriate. The crystal-cleaving picture involves the surface energy,²¹ the energy per unit area required to separate two halves of a macroscopic crystal along a given plane. For the simple-cubic NaCl, the surface energy of a (110) plane is 2.7 times as large as that of a (100) plane.²³ However, the two surface energies can be rationalized by consideration of the density of nearest-neighbor broken bonds which is $\sqrt{2}$ larger for a (110) surface than for a (100) surface. Thus, if the surface of a cluster is viewed as being defined by the surface nearest-neighbor bonds, the bond-breaking and crystal-cleaving pictures are similar. The bond-breaking model somewhat underestimates the relative stability of low-energy surfaces. Still, statistical considerations alone enhance production of low-surface-energy clusters.

The CsI crystal, which is body-centered cubic (bcc) at room temperatures and below, has (110) planes as lowest-surface-energy planes. The intersection of six such planes forms a rhombohedron for which the faces have interior angles 70.5° and 109.5° and the sides meet at 60° and 120° angles.²⁴ An $N \times N \times N$ array of atoms comprising such a crystallite can be viewed as a slightly skewed cube. This structure, we suspect, explains the similar mass spectral intensity anomalies seen at identical n values in simple-cubic and bcc ionic crystals.¹² Martin²⁵ has studied a neutral 24-atom bcc cluster and found that it is an unstable configuration. However, the crystallite that he studied was approximately spherical, thus having high surface energy. Our analysis suggests studying the stability of clusters in a shape of rhombohedra. We have computed the energies of two 27-atom bcc clusters within a simple point-charge ionic model. The first is a $3 \times 3 \times 3$ bcc cluster having six (110) planes and the second is the same cluster except with the ion at one of the corners defined by the

intersection of the facets meeting at 60° removed and placed at the center of a nonadjacent face while the other ions remain fixed. (All the other ions must have their charges reversed in order to stabilize a cluster of the same charge.) Although the latter structure is more spherical, the ratio of total energies is 1.04.

On the basis of these qualitative arguments, we associate the enhanced intensities of CsI cluster ions in Fig. 1 at $n = 13, 22, 37,$ and 62 with low-surface-energy $3 \times 3 \times 3, 3 \times 3 \times 5, 3 \times 5 \times 5,$ and $5 \times 5 \times 5$ rhombohedra. The evidence for enhanced intensities associated with $3 \times 3 \times 7$ and $3 \times 5 \times 7$ structures at $n = 31$ and 52 is less compelling.

This picture of the SIMS sputter-ejection mechanism for ionic crystals has several consequences. It predicts mass-spectral anomalies at identical positions in the distributions of ion intensity versus n for simple-cubic crystals. These have been observed for RbI ($n = 1-16$),¹² KI ($n = 1-22$),¹² and NaI ($n = 1-36$),¹⁷ but higher-mass intensity signals were not detected.^{12,17} On the other hand, this simple picture does not distinguish between positive and negative ions and thus predicts identical intensity anomalies in the negative-ion spectra. However, we have not been able to detect negative ions $[\text{I}(\text{CsI})_n]^-$ greater than $n = 4$ for CsI (Ref. 11) (perhaps because of instrumental limitations), which is the most emissive of the alkali iodides studied (LiI, NaI, KI, RbI, and CsI). The absence of significant ion intensity for large negative-ion clusters may be due to various electron detachment processes.²⁶ This hypothesis can be tested by comparing the ratio of Cs- $(\text{CsI})_n$ and I- $(\text{CsI})_n$ sputtered neutrals.

In conclusion, we have shown that statistics and energy conservation alone favor compact structures for the sputtered cluster ions even in the absence of collisions and other interactions within the selvage region.²⁷ Of course, these other processes do occur, and most readily, on the high surface energy regions of the cluster, thereby further enhancing the number to compact clusters. In any event, we believe that the intensity anomalies seen in Fig. 1 are compelling evidence that the majority of the positive ions observed in SIMS of ionic crystals are compact and that these clusters essentially retain the geometry of the parent crystal.

One of us (T.M.B.) would like to thank the National Research Council for support as a Resident Research Associate. One of us (B.I.D.) thanks J. D. Ganjei, J. S. Murday, and C. T. White for stimulating discussions.

- ¹*Alkali Halide Vapors: Structure; Spectra and Reaction Dynamics*, edited by P. Davidovits and D. L. McFadden (Academic, New York, 1979).
- ²C. M. Rosenblatt, *High Temperature Science: Future Needs and Anticipated Developments* (National Academy of Sciences, Washington, D. C., 1979), p. 23.
- ³M. Blander, in Ref. 1, p. 6.
- ⁴T. P. Martin, *Phys. Rev. B* **15**, 4071 (1977).
- ⁵J. Berkowitz, in Ref. 1, p. 155-188.
- ⁶J. Berkowitz, in *Electron Spectroscopy: Theory, Applications and Techniques*, edited by C. R. Brundle and A. D. Baker (Academic, New York, 1977), Vol. 1, p. 355-433.
- ⁷M. Szymomski, H. Overeijnder, and A. E. DeVries, *Rad. Effects* **36**, 189 (1978).
- ⁸F. Honda, G. M. Lancaster, Y. Fukuda, and J. W. Rabalais, *J. Chem. Phys.* **69**, 4931 (1978).
- ⁹D. O. Welch, O. W. Lazareth, G. J. Dienes, and R. D. Hatcher, *J. Chem. Phys.* **68**, 2159 (1978).
- ¹⁰T. P. Martin, *J. Chem. Phys.* **72**, 3506 (1980).
- ¹¹R. J. Colton, J. E. Campana, T. M. Barlak, J. J. DeCorpo, and J. R. Wyatt, *Rev. Sci. Instrum.* **51**, 1685 (1980).
- ¹²T. M. Barlak, J. E. Campana, R. J. Colton, J. J. DeCorpo, and J. R. Wyatt, to be published.
- ¹³R. Buhl and A. Preisinger, *Surf. Sci.* **47**, 344 (1975).
- ¹⁴M. G. Dowsett, R. M. King, and E. H. C. Parker, *Surf. Sci.* **71**, 541 (1978).
- ¹⁵G. Blaise and A. Nourtier, *Surf. Sci.* **90**, 495 (1979).
- ¹⁶N. Winograd and B. J. Garrison, *Acc. Chem. Res.* **13**, 406 (1980).
- ¹⁷T. M. Barlak, J. R. Wyatt, R. J. Colton, J. J. DeCorpo, and J. E. Campana, unpublished results.
- ¹⁸J. E. Campana, unpublished results.
- ¹⁹G. Staudenmaier, W. O. Hopper, and H. Liebl, *Int. J. Mass. Spectrom. Ion Phys.* **21**, 103 (1976).
- ²⁰J. E. Campana, J. J. DeCorpo, J. R. Wyatt, and R. J. Colton, unpublished results.
- ²¹E. Seitz, *The Modern Theory of Solids* (McGraw-Hill, New York, 1940), p. 76-98.
- ²²S. Kirkpatrick, in *Ill-Condensed Matter*, edited by R. Balian, R. Maynard, and G. Toulouse (North-Holland, Amsterdam, 1979), p. 321-403, and references therein.
- ²³M. Yamada, *Phys. Z.* **24**, 364 (1923), and **25**, 52 (1924).
- ²⁴C. Kittel, *Introduction to Solid State Physics* (Wiley, New York, 1968), p. 20.
- ²⁵T. P. Martin, *J. Chem. Phys.* **69**, 2036 (1978).
- ²⁶L. G. Christophorou, *Atomic and Molecular Radiation Physics* (Wiley-Interscience, New York, 1971), p. 521-553.
- ²⁷P. T. Murray and J. W. Rabalais, *J. Amer. Chem. Soc.* **102**, 1007 (1981).

Stability of Ablatively Accelerated Thin Foils

A. Raven,^(a) H. Azechi, T. Yamanaka, and C. Yamanaka

Institute of Laser Engineering, Osaka University, Suita, Osaka 565, Japan

(Received 17 March 1981)

The stability of ablatively accelerated single-layer and multilayer thin foil targets has been studied by x-ray shadowgraphy and x-ray spectral analysis of the rear target surface. Results show the single-layer foil acceleration to be essentially stable with the disassembly being thermally dominated. An upper limit to Rayleigh-Taylor growth of 1.8 is determined compared to a classical value of 11. Evidence, though, of internal layer mixing in the multilayer target is seen.

PACS numbers: 52.35.Py, 52.55.Mg

One of the topics currently of interest to the field of laser-driven compression is the stability of the targets under ablative acceleration. Such instabilities may arise either from nonuniform laser irradiation or from hydrodynamic instabilities, of which the Rayleigh-Taylor (RT) instability is perhaps the best known. Such instabilities, if they occur, could seriously limit the performance of ablatively driven compression for all but the lowest-aspect-ratio targets. A number of theoretical studies related to this problem have been carried out^{1,2} and some indirect indications

of instability occurring have been seen in ablatively driven implosions.³ However, to date the only direct evidence has been on the inner surface of electron-beam-imploded cylinders.⁴ We present here the results of two experiments to examine the problem of target stability under ablative acceleration. The first involves observing the behavior of a single-layer accelerated target by x-ray backlighting. In contrast to previous optical shadowgraphy measurements⁵ this technique allows the high-density target material to be studied. The use of foil acceleration re-